Optical Engineering

SPIEDigitalLibrary.org/oe

# Space telescope design considerations

Lee Feinberg
Lester Cohen
Bruce Dean
William Hayden
Joseph Howard
Ritva Keski-Kuha

Optical Engineering 51(1), 011006 (January 2012)

# Space telescope design considerations

**Lee Feinberg**
NASA
Code 443, NASA Goddard Space Flight Center
Goddard Space Flight Center
Greenbelt, Maryland 20771
E-mail: Lee.D.Feinberg@nasa.gov

**Lester Cohen**
Harvard-Smithsonian Center for Astrophysics
Cambridge, Massachusetts 02138

**Bruce Dean**
**William Hayden**
**Joseph Howard**
**Ritva Keski-Kuha**
NASA
Code 443, NASA Goddard Space Flight Center
Goddard Space Flight Center
Greenbelt, Maryland 20771

**Abstract.** The design considerations for astronomical space telescopes cover many disciplines but can be simplified into two overarching constraints: the desire to maximize science while adhering to budgetary constraints. More than ever, understanding the cost implications up front will be critical to success. Science performance can be translated into a set of simple performance metrics that set the requirements for design options. Cost is typically estimated by considering mass, complexity, technology maturity, and heritage. With this in mind, we survey the many diverse design considerations for a space telescope and, where appropriate, relate them to these basic performance metrics. In so doing, we hope to provide a roadmap for future space telescope designers on how best to optimize the design to maximize science and minimize total cost.  [DOI: 10.1117/1.OE.51.1.011006]

Subject terms: space telescope; James Webb Space Telescope; optical telescope element; Hubble Space Telescope.

Paper 110674SS received Jun. 17, 2011; revised manuscript received Sep. 27, 2011; accepted for publication Oct. 5, 2011; published online Feb. 6, 2012.

## 1 Introduction

Astronomical space telescope design considerations begin with a set of basic science objectives that are translated into high-level performance metrics. These metrics, which typically include field of view, diffraction-limited performance, and sensitivity, are the key design considerations. The design process then results in a cost, thus yielding a basic relationship between the cost and science of the mission. If the cost is unaffordable for the given science, the science requirements can be reduced and a new science-to-cost relationship established. The connection between science and performance and then cost is the ultimate relationship governing the design of a space telescope. In earlier studies,[1,2] data regarding light- and information-gathering power versus cost of photometric telescopes of various sizes have been examined. But at a more conceptual level, the cost-to-science ratio for typical space telescope missions is illustrated in Fig. 1. Successful missions typically fall into a basic band shown in gray. Missions that have narrow science objectives at high costs typically do not get off the ground. These missions would fall outside the gray band. A key consideration is that many missions grow in cost as they are better understood, so ensuring that the original design has margin in this basic ratio is key to ensuring its successful completion.

In this paper, we survey the design considerations that connect the basic science objectives to cost and performance. For each type of key design consideration, we summarize the basic trade-offs to consider with the basic generic metrics or considerations. Every space telescope is unique in the specific trade-offs, but these top-level trade-offs and considerations serve as a roadmap for future astronomical space telescope designers. These trade-offs ultimately reduce to performance (and thus science) or cost drivers (mass, complexity, technology maturity, etc.), and instruct system architects on the key considerations to ensure they can stay in the success band.

This somewhat subjective representation is really aimed at highlighting the importance of maintaining science capabilities proportionate to cost. While smaller missions do fall along this proportional curve, this paper is aimed at challenges with major space telescope observatories and uses the James Webb Space Telescope (JWST) as a key example throughout. Besides total cost, availability of funding is also an important parameter that ultimately impacts the total cost through program stretch-outs. Avoiding large cost overruns is best accomplished by estimating costs properly up front. While it is difficult to guess what a technologically complex system will cost, it relates directly to the architectural complexity discussed in this paper.

## 2 Architecture Considerations

In general, the design of a space telescope starts with the definition of basic optical design parameters: field of view, diffraction-limited wavelength, sensitivity (and thus aperture size), and wavelength sensitivity. Typically, multiple architectures are developed that are traded against each other. Even after a basic architecture is selected, the design will continue to evolve, usually due to cost realities and often toward smaller apertures. In the end, the goal is to maximize science and the key constraint is cost.

The first of the optical design parameters that typically drives the overall architecture is the size of the primary mirror (PM). Once the clear aperture is determined, the first basic trade-off is whether a monolith of segmented architecture will be used. To first order, this is a simple trade-off driven largely by the size though diffraction-limited wavelength and sensitivity-driven temperature can also matter. A survey of historical missions and proposed missions shows that the cutoff for a monolith is typically at 4 m due to the rocket shroud size and mass limitations. A subtlety of this trade-off is that a key simplification offered by the monolith design

0091-3286/2012/$25.00 

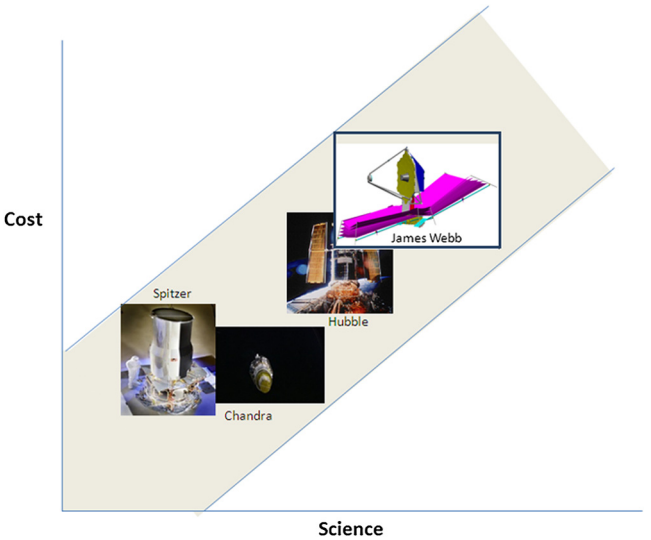


**Fig. 1** Cost versus science ratio of major observatories.

is the ability to have a fixed baffle tube to avoid the sunshield complexities of an open architecture. However, the baffle tube needs to be designed to avoid contacting the PM or rocket during launch so a near meter–diameter penalty is paid for the monolith design to accommodate the baffle tube. This cutoff size could move up if a new, large, and cost-effective class of rocket shroud is developed. However, keep in mind that several successful launches need to be proven before a space telescope can confidently use a new rocket.

Assuming that a segmented telescope is adopted due to the size, the next question is the orbit. At a simple level, the closer to Earth the lower the cost to get to orbit, so low earth orbit (LEO) is the cheapest followed by geostationary orbit and by the L2 Lagrange point. However, LEO has several cost and performance implications ranging from the large thermal swings resulting from occultations to the communication and scheduling challenges of occultations. For open telescopes that do not have a baffle like the JWST, LEO is not compatible with the stray light and thermal background.

As shown in Fig. 2, many NASA future missions have adopted L2 as the desirable location. The moon is also a consideration but has the challenges of landing loads, dust, and accessibility to optimal locations like the poles. L2 still has the challenge of serviceability, although robotic servicing developed for the Hubble Space Telescope (HST) demonstrated the potential of this approach for L2.

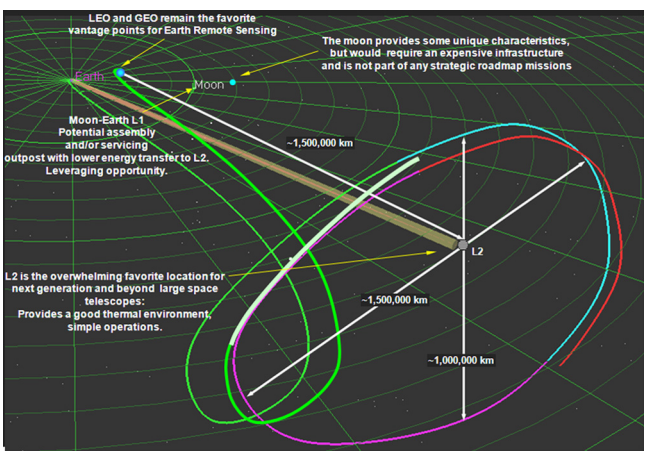


**Fig. 2** Vantage point options.

A related trade-off is whether the telescope will be deployed or assembled and/or serviceable. Assembling a telescope in space requires a large up-front expense and impacts mass availability so most proposed telescopes that can be fit into a single rocket are proposed to be deployed. The 2005 Advanced Telescope and Observatory Study concluded that serviceability is the first requirement for L2.[3]

The other major decision that ripples through an architecture is the trade-off of passive or active (or adaptive) control of the PM. Being cryogenic and the first segmented telescope, JWST went with an active align-and-forget architecture capable of periodic adjustments. However, room-temperature telescopes with tighter performance requirements like advanced technology large-aperture space telescope (ATLAST) and terrestrial planet finder coronograph (TPFC) benefit from various levels of active or even adaptive control.

## 3 Optical Design Considerations

Both the field-of-view and image quality requirements for the desired mission have an influence on the optical design of space telescopes. In general, as the field of view increases, an increasing number of powered mirrors are necessary to meet the specified image quality requirements. Sensitivity also can influence a design choice, where every reflection or transmission through glass has a significant degradation on system throughput, thus pushing the design toward fewer surfaces. The cost is determined by the design but is generally driven by performance needs.

The simplest focusing telescope (or camera) is a single mirror, typically used for a very narrow field system. One example is the Far Ultraviolet Spectroscopic Explorer (FUSE), in which light from a very narrow field is focused onto a series of slits that feed a Rowland circle spectrograph. The sensitivity needs for this mission required minimal reflecting surfaces, in this case only a single focusing off-axis parabola (OAP) for each of its focusing channels. This single-mirror telescope design yields stigmatic imaging at the focus of the parabola, but like all Newtonian telescopes, the image quality degrades linearly with field angle since coma is uncorrected.

As more powered mirrors are added to a telescope design, additional degrees of freedom are provided to remove aberrations and improve image quality. In general, each powered mirror provides correction for a single third-order aberration. A single-mirror system can correct spherical aberration (i.e., OAP design), but coma and astigmatism remain, both of which cause blur off-axis. A two-mirror system, on the other hand, can be designed to be free of both spherical aberration and coma [i.e., Ritchey-Chretien design (RC)], leaving only astigmatism as a blurring influence on the image quality. The two-mirror design was adopted for the HST where proper correction allows for reasonable imaging across several arcminutes of field of view. A three-mirror system provides correction of third-order spherical aberration, coma, and astigmatism, allowing for fields of view of 20 arcmin (e.g., JWST) and up to several degrees [e.g., the Wide-Field Infrared Survey Telescope (WFIRST)]. These designs are referred to as "Korsch three-mirror anastigmats" (TMAs), and are

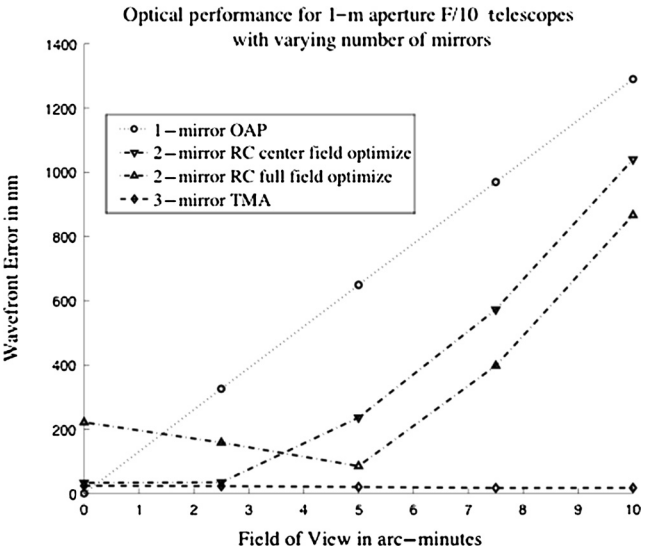


**Fig. 3** Examples of one-, two-, and three-mirror systems (i.e., FUSE, HST, and JWST, respectively).

becoming more common as science demands larger fields of view for consideration. A fourth mirror can be added to further correct the field, or even allow third-order distortion to be corrected, which is very useful for scanning or "push-broom" type systems.

Figure 3 illustrates how increasing the number of powered mirrors will improve image quality for a given system. Four plots are included in the figure, comparing image quality performance in wavefront error (nanometer units) versus field of view from the center-field point. For direct comparison, each telescope has a 1-m aperture and a 10-m focal length (i.e., $f/10$ system). As expected, the single-mirror-system image quality degrades rapidly with field, and the degradation is linear since coma dominates OAP performance. Two RC designs are plotted, one which has been optimized for the center of the field, and the other for the entire field. The center-field—optimized RC performs nearly as well as the OAP at the center, but it retains good performance out to about 3 arcmin before it starts to degrade quadratically in field (i.e., dominated by astigmatism). The full-field optimized RC shows that you can get better performance further

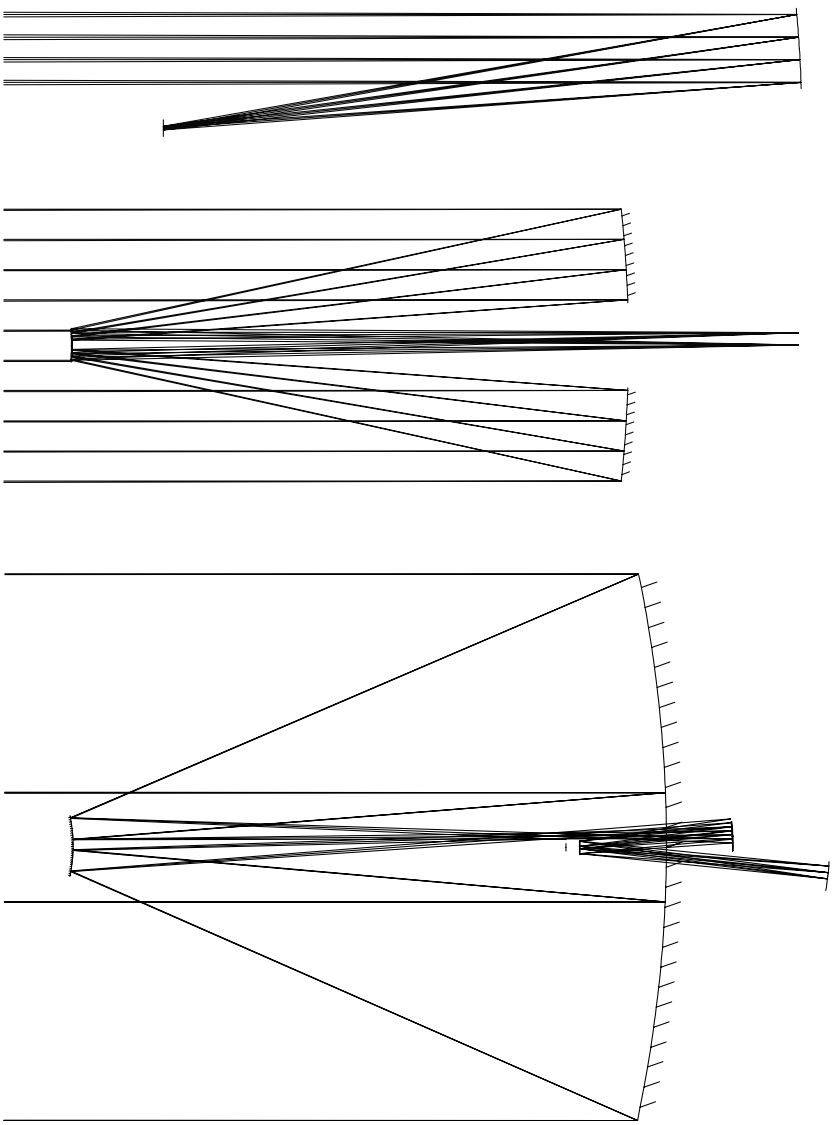

**Fig. 4** Drawings of one- , two- , and three-mirror focusing telescope designs.

in the field, in this case out to 5 arcmin, but at the cost of center-field performance. Finally, the TMA in this study performs extremely well past 10 arcmin from the center of the field. A summary of the configuration options is shown in Fig. 4. Although not to relative scale, the single mirror is similar to the FUSE mission, the two-mirror is similar to the HST, and the three-mirror design is similar to the JWST.

In general, three-mirror systems are also more tolerant of misalignment since they are corrected for the third-order image blur aberrations. When the secondary mirror (SM) is decentered by 10 μm, for example, the two-mirror system shown in Fig. 4 degrades by ~24 nm RMS wavefront error (WFE), whereas the three-mirror system degrades by only ~8 nm RMS WFE.

## 4 Optomechanical Considerations

Once an optical design is selected, the next step is the optomechanical design. Most optics for use in space can be approximated as circular flat disks for initial sizing consideration including fabrication costs, manufacturing effects related to strength and stability, stiffness related to launch strength, test and on-orbit vibration effects, test and in-use thermal and temporal stability, and finally, effects of assembly. The use of the first free-free natural frequency as a basic metric for optic stiffness is widely accepted and is proportional to $K[(Dg/wr^4)]^{1/2}$ where: $K$ is related to the mode number, $D$ is the flexural rigidity of a uniformly thick disk $(Et^3/12(1-\nu^2)$, where $E =$ modulus of elasticity, $t =$ thickness, and $\nu =$ Poisson's ratio), $g$ is the unit value of acceleration (e.g., 9.8 $m/s^2$), $w$ is the mass per unit thickness of the disk, and $r$ is the disk radius. From this it can be seen that as the radius increases, the first frequency decreases by the increase in $r^2$. The frequency also decreases with increased areal mass ($w$) but by only $w^{1/2}$, and as the disk becomes uniformly thicker, including its areal mass, the frequency increases linearly with thickness ($t$). There is no single metric for optic stiffness that can or should be used to derive a single design. The topics noted above interact with one another but it is always true that the stiffer an optic is the more it will resist stress caused by environments and material instabilities. Almost all large space optics are light-weight and utilize open-back, closed-back, or semi-closed-back designs, and are usually classified as rigid or semi-rigid. These latter classifications define the optic's ability to be corrected by its support system for very-low-order optical errors. The equivalent mechanical properties for the light-weight rigid and semi-rigid designs can be determined[4] and used with the above equations.

Low-rigidity or flexible optics may have some level of light-weighting but not nearly as much as those discussed above. These optics can be adjusted to correct for many optical aberrations caused by manufacturing, assembly errors, mount deformations, and so on. The more flexible an optic is, the more flexible its support system has to be if it is going to be corrected with that support system. A rigid mirror that does not require rigid body alignment after assembly into its metering structure can have a support system that is very stiff (but must accommodate compliance for any thermal or other temporal strain). On the other hand, a thin meniscus mirror that has 50 figure actuators attached to its back must consider the required flexibility of each actuator and the motion that each must undergo. In the JWST case, the low-authority design was found to have one third lower areal density than a moderate-authority architecture, while a high-authority design was found to be about one third the areal density of the low-authority mirror. However, those ratios can vary depending on actuator type and mirror specifics.

The JWST primary mirror segment assembly (PMSA) allows the beryllium (Be) mirror to be adjusted in six nearly rigid-body motions and also allows its radius of curvature to be changed. The rigid-body motion is accomplished via a hexapod actuator system, which has internal flexures to minimize the forces and moments imparted to the mirror. The JWST design utilizes 18 hexagonal segments, even though it could have also utilized 36 stiffer hexagonal segments. However, manufacturing costs, optical and mechanical test costs, transportation costs, and polishing challenges like edges drove the choice of fewer less stiff but "stiff enough" segments.

**Table 1** Listed here are the material properties for mirror substrates in operating and test environments.

| Material | Density $\rho$ ($kg/m^3$) | Young's modulus $E$ (GPa) | Specific stiffness $E/\rho$ (m) | Nominal design allowable stress $\sigma$ (MPa) | CTE at 293 K (PPM/K) | CTE at 40 K (PPM/K) |
|---|---|---|---|---|---|---|
| Borosilicate | 2230 | 63 | 0.028 | 10 | 3.3 | –3.2 |
| Fused silica | 2200 | 73 | 0.033 | 10 | 0.5 | –0.7 |
| ULE® | 2210 | 68 | 0.031 | 10 | 0.03 | –0.7 |
| Zerodur | 2530 | 91 | 0.036 | 10 | 0.05 | –0.7 |
| CVD SiC | 3210 | 466 | 0.145 | 138 | 2.2 | 0.05 |
| Reaction-bonded SiC | 2910 | 360 | 0.124 | 69 | 2.4 | 0.02 |
| O-30 beryllium | 1850 | 300 | 0.162 | 13 | 11 | 0.05 |
| Aluminum | 2700 | 70 | 0.026 | 69 | 23 | 2.5 |

*Note:* Nominal design stresses are allowed based upon minimizing residual figure error from over-stressing the part. Actual CTE in the vicinity of 40 K can vary from the tabulated values. The specific stiffness parameter is a general metric to show which materials provide the highest stiffness to weight ratio. CVD, chemical vapor deposition; CTE, coefficient of thermal expansion.

**Table 2** Listed here is the steady state thermal distortion index for rating material deformation at room and cryogenic temperatures

| | Reaction | | | | | |
|---|---|---|---|---|---|---|
| | Beryllium | | Bonded silicon carbide | | Fused quartz | |
| Property | 10 K | 293 K | 10 K | 293 K | 10 K | 293 K |
| Coefficient of thermal expansion, $\alpha$ (ppm/K) | 0.001 | 11.3 | 0.015″ | 2.6 | −0.26 | 0.50 |
| Thermal conductivity, $k$ (W/m K) | 37 | 216 | 300″ | 155 | 0.11 | 1.4 |
| Specific heat, $C_P$ (W s/kg K) | 0.39 | 1925 | 0.1[a] | 670 | 4.0 | 750 |
| Steady state distortion coefficient, $a/k$ (um/W) | 0.001 | 0.052 | 0.001 | 0.017 | 2.4 | 0.36 |
| Density, $p$ (g/cm$^3$) | 1.850 | | 2.89 | | 2.19 | |
| Young's modulus, $E$ (GPa) | 287 | | 330 | | 74.5 | |
| Self-deflective: equal mass, $E/p^3$ (arbitrary) | 45 | | 14 | | 7 | |
| Total contraction, 293 to 10 K (ppm) | 1298 | | 350″ | | −50 | |

[a]Estimated.

Choosing the proper mirror substrate material for the operating and test environments is key to mission success. Table 1 was amended to incorporate additional material.[5] The table shows the specific stiffness metric (stiffness to density ratio) along with other pertinent material properties. Table 2 shows the steady-state thermal distortion index (along with other useful material properties),[6] which is used to rate how material will deform at room temperature (293 K) and at cryogenic temperatures (10 K). Note in Table 2 that at cryogenic temperatures, Be had a much lower index than fused quartz (which has an index similar to ultra-low expansion glass, ULE®) and also that its specific stiffness was the highest of all of the materials in Table 1. These were the primary technical reasons that Be was chosen over ULE for the JWST mirrors. At or near 293 K, ULE, fused silica, or Zerodur® would have been a much closer competitor to Be using the distortion index.

## 5 Coatings

A key factor in optimizing the throughput of a space telescope is selection of the optical coating for the mirrors. The operating wavelength range of the mission is the key consideration in selecting the coating. Since every telescope is unique, the coating needs to be tailored to the specific application. However, in general to maximize throughput, the reflectivity of the coating should be as high as possible, typically over a broad wavelength range. Additionally, the coating process and the material have to be compatible with the size of the optic and the substrate material. The coating needs to survive the environmental conditions the telescope is exposed to on the ground, usually for several years before launch, as well as on orbit. The following paragraphs discuss some of the most commonly used coatings in different wavelength ranges.

Magnesium fluoride ($MgF_2$)–protected aluminum is the most commonly used coating in the vacuum, ultraviolet spectral region because of its high reflectivity down to 110 nm. This coating is used on HST optics covering the wavelength range from 110 nm to near IR. $MgF_2$–protected aluminum is a soft coating that scratches easily. Therefore, optical components with this coating have to be handled carefully to avoid damage to the coating. Cleaning should be attempted only in emergency situations. $MgF_2$–protected aluminum coating has to be deposited quickly in high vacuum to avoid oxidation of the aluminum and thereby loss of performance. Lithium fluoride overcoating can extend the useful range of aluminum down to the LiF absorption cutoff of 102.5 nm. Unlike $MgF_2$ overcoating, which affords excellent protection and long life, LiF overcoating is hygroscopic and exhibits reflectance degradation and increased scatter with age. In the wavelength region below 102.5 nm, all conventional coatings have low reflectivity.[7]

In the spectral region above 200 nm through the visible range, evaporated aluminum protected by a $SiO_x$ overcoating provides a high-reflectivity, stable optical coating. It is also used in far-IR and microwave wavelength regions. For example, the Herschel 3.5-m diameter SiC mirror and WMAP composite mirrors are coated with aluminum with a thick $SiO_x$ overcoating. For applications above 600 nm through the IR, protected evaporated gold provides high reflectivity and robust coating. This is the coating of choice for the JWST PMSA's secondary and tertiary mirrors as well as the fine steering mirror (FSM). The wavelength range of JWST is from 800 nm to 29 μm.

In applications where higher reflectivity below 600 nm is required, protected silver can provide high reflectivity down to 400 nm. This coating was considered for the JWST telescope; however, protected silver is not as robust as protected gold. Protected silver is a commonly used coating in applications where high reflectivity is required down to 400 nm. For example, the HST advanced camera (AC), long-wavelength channel optics are coated with protected silver. Since JWST's science does not require high throughput below 800 nm, protected gold was selected over protected silver. Electroplated gold is also used for IR applications on metal mirrors.

## 6 Wavefront Sensing and Control

An important technology for helping to improve the cost versus science return is wavefront sensing and control (WFSC). In simplest terms, WFSC is a relatively new tool for mission systems designers: by introducing optical degrees of freedom into a telescope design, early in the design stages, the system architect can make use of light-weight mirrors and structures through active control, translating into overall savings in system mass and cost. It also enables telescopes too large to launch in available fairings to do so by providing the ability to align relatively loosely deployed optics into a diffraction-limited optical system. Since science return often correlates to aperture size, the trend in telescope design is for increasing aperture diameter while constraining overall telescope mass to launch vehicle requirements. For example, JWST launch vehicle constraints[8] dictate a segmented PM with an area of 25 $m^2$, areal density[9] of less than 25 $kg/m^2$, and a deployable SM. To meet science requirements, the PM design is based on a 6.5-m, 18-segment hexagonal array using O-30 grade Be[10] for cryogenic stability at the anticipated orbit about L2. (The telescope is designed for operation over a temperature range of 30 to 60 K.) As a result of these deployment and thermal stability constraints, the JWST commissioning and periodic optical maintenance must be accomplished using an active optical control system, or WFSC.

In addition to increasing the science return versus cost ratio, WFSC reduces mission risk by allowing the telescope to recover from unintended deployment states, and by utilizing optical correction by way of adjusting component shapes and position. The importance of including a WFSC subsystem early in the design stages of a space telescope was realized even before the launch of Hubble. Large telescopes (greater than approximately 4 m) dictate that the observatory must be stowed before launch, and thus intermediate-unpacking stages must be used to commission the telescope. A typical WFSC subsystem designed for this task is illustrated in Fig. 5, which shows the chronological order of the JWST commissioning steps. In summary, the JWST commissioning steps follow:

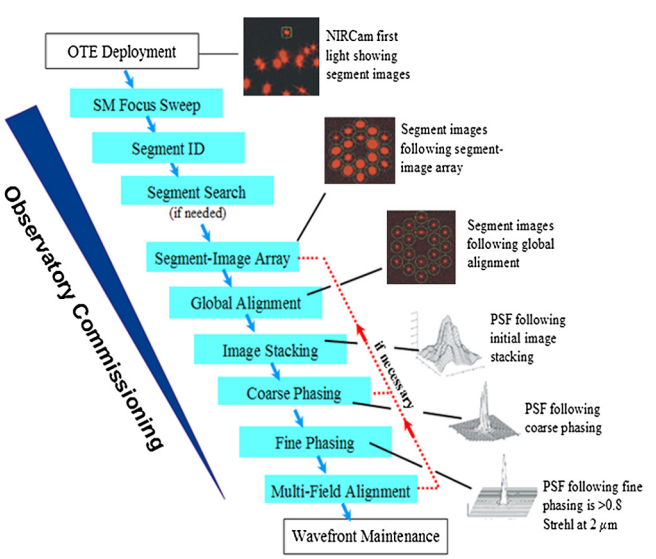


**Fig. 5** Block diagram of WFSC steps.

1. SM focus sweep: The SM focus sweep algorithm finds an initial position for the SM.
2. Segment ID: The segment identification algorithm determines the location for each of the 18 PMSA images.
3. Segment search: The segment search algorithm locates missing segments not found during the segment ID process.
4. Image array: The segment-image array algorithm moves segment images into a predetermined hexagonal image array of the mirror segments in preparation for global alignment.
5. Global alignment: The global alignment algorithm generates individual segment wavefront maps that are used to more accurately position the SM.
6. Image stacking: The image stacking algorithm co-aligns the individual segment images in preparation for coarse phasing.
7. Coarse phasing: The coarse phasing algorithm decreases the WFE in the PM by adjusting each PMSA piston value.
8. First is the fine-phasing (phase retrieval): The fine-phasing algorithm makes final adjustments to the positions of the SM and PM segments to meet the telescope's WFE performance requirement. Next is multifield fine-phasing: fine-align the SM, and then wavefront maintenance will use both fine-phasing steps as required.

In the commissioning process, sensors providing feedback are needed to guide deployment. To further leverage cost and maximize science return, it is desirable to have the science camera double as the wavefront sensor. This constraint dictates that an image-based wavefront sensor be deployed for the final stages of commissioning. Typically, this is handled using a phase retrieval step,[11] which is more cost effective that installing a Shack–Hartmann subsystem. Technology Readiness Level (TRL)-6 results have been reported for JWST commissioning steps in the literature.[12]

Beyond phase retrieval, several other technologies are needed to enable a better science-to-cost ratio. For example, architectures based on a deployable PM require translation alignment (piston) between segments. This "coarse" alignment procedure has been developed under the JWST test program as a variant on white-light interferometry, by using a dispersed Hartmann sensor (DHS),[13] a simple grism-based optical component. A flight-like article was produced by Adaptive Optics Associates (AOA) and was thoroughly tested to assess survivability and optical performance. Other variations on the device have been considered such as the dispersed fringe sensor (DFS).[14,15] Both approaches have been tested[15] on the Keck Observatory telescope system. Early in the program, a trade-off study[16] was conducted by the JWST project to assess advantages and disadvantages for each of the DHS and DFS methods. It was determined that the DHS approach was the best overall method for flight, based on cost, deployment time, and risk assessment. For further comparison, the Keck employs a capacitive-based edge sensor for piston detection phasing camera system (PCS) and rather than phase retrieval for *in situ* figure control (fine-phasing), the Keck design uses a warping harness to set

the correct shape by applying forces to the segment back at 36 points.[17]

## 7 Systems Issues

Addressed here are the systems engineering aspects to optical, thermal, and stray light performance, and system testing. In order to achieve the science objectives, a systematic budgeting process is needed to decompose the science requirements into engineering terms. These budgets provide the structure to trade-off architecture options, as well as defining where the interfaces must be. Performance and resource budgets are used to systematically allocate requirements and resources, to target technology development, to identify trade-off studies, and to manage interfaces and requirements. Another useful aspect of the budgets is to manage the margin. Margin can be loosely defined as the sum of reserve, explicit margins held at various levels, and conservative factors such as modeling uncertainty factors (MUF). This gives the project the flexibility to reallocate this margin as the system design matures, or if there is a need to accept more risk by explicitly accepting lower MUF, or if achieving stated requirements will have unacceptably high cost, or if testing presents large uncertainties in performance verification. Ultimately, proving that the telescope meets its requirements by test and/or analysis is the final systems issue.

Although not addressed here, the HST and the Space Station have demonstrated that servicing can be an effective life-cycle option. Currently, LEO orbits are the only orbits where this is possible. Human-rating a system is costly, as well as an astronaut-attended servicing mission, whereas robotic servicing has real potential for near-Earth servicing of space telescopes. Of course, this technology development needs to be included in the life-cycle costs of a space telescope. If there is an option to service, a project team may be willing to accept higher performance risks that can lead to lower costs.

The technological status of options is a key cost driver, and full life-cycle costs to implement these are difficult to estimate but important cost drivers. Having a systematic approach to validating technology is essential to controlling cost and schedule, for which the NASA technology readiness level (TRL) process has been developed.[18] The performance budgets establish the framework for trade-off studies to deal with technology limits. For example, if a telescope needs on-orbit alignment capability to deal with deployment or cryogenic operations, trade-off studies can determine the degrees of control freedom for the mirrors based on the technological limits of precision structures, mirror materials, and high-resolution actuators, or conversely to identify where those limits need to be pushed with targeted investments. Seven degrees of freedom in the form of hexapods plus radius of curvature control were chosen on JWST to enable the compensation of potential errors such as mirror segment power and astigmatism, prescription registration, and drift or slip in the alignment. From this analysis, light-weight, semi-flexible mirrors, precision cryogenic actuators, and cryogenic electronics became investments with prescribed achievement gates as part of the development life cycle.

The WFE budget is an excellent way to manage optical performance, even if Strehl or encircled energy are the primary science parameters—WFE is an industry standard metric for manufacturing optics, and there are reliable techniques for combining WFE from all the optics and environmental effects such as jitter and misalignments. In the case of an active optical system, sensing and control effects on WFE need to be included, which by design attenuate many of the WFE contributions to a telescope. Making the WFE budget as detailed as possible, down to the level of each optical component, including manufacturing, coating, jitter, drift, and thermal/cryogenic effects allows this tool to effectively control requirements, interfaces, and margin. Creating specifications naturally flows from this tool. And as parts are built and tested, it enables tracking the give and take of margin.

Budgets for throughput, contamination, collecting area, and in the case of active optics, actuator resolution, and range, directly impact the optical architecture and detailed design. Other budgets that impact the telescope architecture and detailed design are power, mass, and thermal. Most telescopes need tight thermal control, or operate at cryogenic temperatures to support IR science; hence the thermal design often requires significant systems and discipline engineering.

The thermal subsystem for a telescope that operates in the IR is likely a major investment. Passive or active thermal control is a fundamental trade-off. JWST chose to passively cool the telescope and the near-IR instruments, but actively cool the mid-IR instrument with a cryo-cooler due to the technology and cost limitations of actively cooling a large and massive telescope. As with other systems areas, a detailed performance budget, grounded with detailed analysis, component and subscale testing, and adequate margin, are essential for achieving science performance. Validation testing and subsystem integration and test (I&T) can be major cost drivers but are critical due to the workmanship-sensitive nature of both passive and active thermal control systems. From an optical perspective, choosing materials with known cryo properties and low coefficient of thermal expansion (CTE) are necessary for achieving stability. The thermal and thermal–mechanical modeling needs to be well-planned and sufficiently funded. Thermal stability is one of the major drivers in the trade-off for a passive, active, or adaptive telescope. It also drives operational constraints for pointing, stabilization time, image integration time, and the frequency of WFSC. The investment in this subsystem can have large payoffs in other subsystems and operations.

A key driver for instrument sensitivity is stray light, which is dominated by baffle design, temperatures, and contamination. Stray light is irradiance from unintended light paths, thermal self-emission, and radiation-induced self-emission.[19] Figure 6, from JWST, illustrates the different sources of stray light compared to the galactic background. Baffle design requirements are highly coupled with aspects of contamination control—a well-baffled telescope reduces the solid angle exposure of contaminated optics. Apart from stray light, contamination also reduces the throughput of the optics, further impacting sensitivity.

Unless the telescope optics are perfectly clean, smooth, and cold, and all nonoptical surfaces are perfect light absorbers and sufficiently cold, some form of baffling is required. However, deploying a well-baffled, large space telescope can create more problems than it solves, leaving a partially baffled telescope like JWST as the best design option. This exposes more of the optics and structure to background light, which in turn drives the particulate and molecular

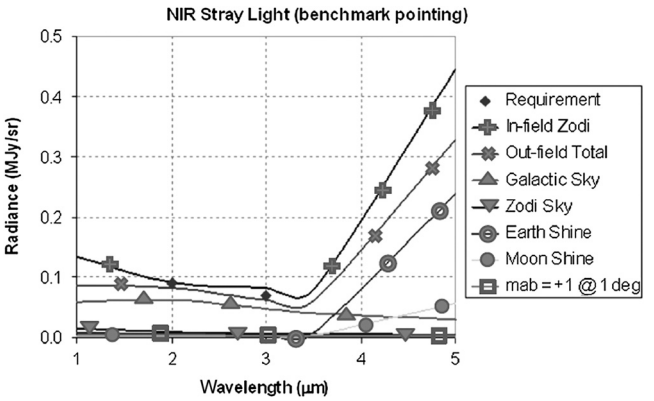


**Fig. 6** JWST stray light performance.

contamination requirements for all surfaces. A highly compact telescope design is susceptible to obscure stray light paths. On JWST, two particular stray light paths triggered additional design and alignment requirements. The first was a direct path that entered the system via the Cassegrain focal surface mask. The second path came from any bright source at the edge of the unbaffled PM as viewed from the SM. The solutions to these were very accurate baffle design and pupil alignment with targeted testing for verification.

Stray light analysis is notorious for inaccuracies due to modeling surface properties, particularly the bidirectional reflectance-distribution function (BRDF), data uncertainties from extrapolations across wavelengths, and various distributions of particulates. Verifying by test at all angles and all wavelengths is difficult, so verifying stray light by analysis is often undertaken. To ensure compliance with the requirements, a 10× margin should be the goal, and if compliance is essential, two independent models anchored as much as possible with test data should also be built. Using three-dimensional visualization adds the capability to "fly" through the stray light design to find unintended gaps in the baffles or unintended structure in the light path.

Mid-IR is dominated by thermal self-emissions, so temperature and thermal properties of materials need to be design parameters. This adds an additional, often conflicting, layer of requirements to the thermal control system.

A detailed contamination control budget enables the contamination management of the telescope. This budget must be based on end-of-life particulate and molecular requirements derived from stray light, optical throughput, and thermal performance requirements. The budget is then suballocated to cleanliness at each relevant gate in the ground processing life cycle, such as delivery of the mirrors from the vendor and I&T, and it also includes allocations for on-orbit sources of contamination such as desorbed moisture, outgassed molecular material, UV polymerized molecular accumulations, and micrometeoroid damage. This budget will flow cleanliness requirements to the pertinent subsystems, to the test and storage facilities, and to the launch site. This then spawns contamination-monitoring plans, contamination models, and inputs for the stray light, optical throughput, and thermal models. Cleaning the mirrors later in the I&T phase is a method for increasing or recovering margin.

The last system consideration is testing of the telescope. Earlier generations of space telescopes were verified by test. JWST with its semirigid 6.5-m PM will be a hybrid of verification by test and by analysis. Eventually telescopes will be built that cannot be tested on the ground as a single assembly. The telescope project must make the investment in adequate detailed modeling and simulation to verify the full system via analysis before launch. To some degree, the ability to build and test a subsystem for flight has already been demonstrated with all of the science instrument upgrades flown on HST. Moreover, the Space Station has demonstrated that large structures can be assembled in space. Early in the design, it must be ensured that the architecture is robust and the interfaces are well defined. This means sufficient degrees of freedom and sufficient deployment ranges so that subsystems can be verified individually before installation. The break point for telescopes that cannot be tested on the ground is around 10 m. The break point is also dictated by how large a structure can be transported, so both deployed and stowed configurations drive this decision. A key point is that testing and even shipping space telescopes is often an afterthought, but with larger telescopes this has become a major cost driver. It is critical that the architecture accommodate testing needs up front. A small investment in adequate degrees of freedom, and sufficient deployment and control range can help prevent large cost escalations in the test program.

## 8 Conclusion

In summary, the basic design considerations for large astronomical type telescopes have been described. While cost is a major consideration, cost is driven by complexity and risk in the form of metrics and technical challenges that have been outlined in this paper. Each telescope is different and requires its own set of considerations. However, usually there are just a few key technological drivers for a given architecture and many of the other design considerations flow from there. In other words, this paper is only a top-level guide and each individual design requires its own very detailed considerations.

### *References*

1. H. L. Johnson and W. L. Richards, "Optimum size of infrared photometric telescopes," *Astrophys. J.* **160**(2), L111–L116 (1970).
2. J. Oke, "On the optimum size of optical telescopes," *Astrophys. J.* **162** (2), L77–L78 (1970).
3. National Aeronautics and Space Administration, *Advanced Telescope and Observatory Capability Roadmap*, NASA, Washington, DC (2005).
4. K. Doyle, *Integrated Optomechanical Analysis*, SPIE Press, Bellingham, WA (2002).
5. P. Bely, *The Design and Construction of Large Optical Telescopes*, Springer, New York (2002).
6. D. Coulter, S. A. Macenka, M. T. Stier, and R. A. Paquin, "ITTT: a state-of-the-art ultra-lightweight all-be telescope," JPL Tech Report 97-0827 (2001).
7. R. A. M. Keski-Kuha, et al., "High-reflectance coatings and materials for the extreme ultraviolet," *Proc. SPIE* **2428**, 294 (1995).
8. J. Nella, et al., "James Webb Space Telescope (JWST) observatory architecture and performance," AIAA-2004-5986, American Institute of Aeronautics and Astronautics, San Diego, CA, September 28–30, 2004 (2004).
9. S. E. Kendrick, D. Chaney, and R. J. Brown, "Optical characterization of the beryllium semi-rigid AMSD mirror assembly," *Proc. SPIE* **5180**, 180–187 (2004).
10. T. B. Parsonage, "JWST beryllium telescope: material and substrate fabrication," *Proc. SPIE* **5494**, 39–48 (2004).
11. B. H. Dean, D. L. Aronstein, J. S. Smith, R. Shiri, and D. S. Acton, "Phase retrieval algorithm for JWST flight and testbed telescope," *Proc. SPIE* **6265**, 626511 (2006).
12. L. D. Feinberg, et al., "TRL-6 for JWST wavefront sensing and control," *Proc. SPIE* **6687**, 668708 (2007).

13. M. Albanese, A. Wirth, A. Jankevics, T. Gonsiorowski, C. Ohara, F. Shi, M. Troy, G. Chanan, and S. Acton, "Verification of the James Webb Space Telescope coarse phase sensor using the Keck Telescope," *Proc. SPIE* **6265**, (2006).
14. F. Shi, D. C. Redding, J. J. Green, and C. M. Ohara, "Performance of segmented mirror coarse phasing with a dispersed fringe sensor: modeling and simulations," *Proc. SPIE* **5487**, 897 (2004).
15. F. Shi, C. M. Ohara, G. Chanan, M. Troy, and D. C. Redding, "Experimental verification of dispersed fringe sensing as a segment-phasing technique using the Keck Telescope," *Proc. SPIE* **5489**, 1061 (2004).
16. J. Oschmann, et al., "DHS/DFS independent design review summary and disposition," *Ball Systems Engineering Report*, March (2005).
17. C. Neyman, R. Flicker, and S. Panteleev, "Effect of Keck segment figure errors on Keck AO performance," Keck Adaptive Optics Note 469, W. M. Keck Observatory, Kamuela, HI, March 7 (2007).
18. John C. Mankins, *Advanced Concepts Office of Space Access and Technology*, NASA, http://www.hq.nasa.gov/office/codeq/trl/.
19. J. R. Denison, R. Hoffmann, J. Dekany, A. Evans, C. Sim, A. Sim, J. Hodges, and J. Tippets, "Preliminary assessment of electron-induced electrostatic breakdown and luminescence of JWST materials," Utah State University, NASA Grant NNX08AK01G (2010).

**Lee Feinberg** is the NASA Optical Telescope Element manager for the James Webb Space Telescope and the chief large-optics systems engineer in the Instrument Systems and Technology Directorate at the Goddard Space Flight Center in Greenbelt, Maryland. He is an SPIE Fellow and spent a decade working on the optical correction and instruments for the Hubble Space Telescope. In 1998, he received an MS in applied physics from Johns Hopkins University and in 1987 graduated with a BS in optics from the University of Rochester.

**Lester Cohen** is currently the chief engineer of structural analysis and design at the Harvard-Smithsonian Center for Astrophysics (CfA). For the past decade, he has worked as the James Webb Space Telescope Optical Telescope lead telescope mechanical engineer through a cooperative agreement with NASA Goddard Space Flight Center. Prior to his work on JWST, Lester worked on the Chandra Mission Support Team at the CfA overseeing mirror fabrication and structures work for the high-resolution mirror assembly. He holds a BS and MS in civil engineering. In 2009, he received the NASA Distinguished Public Service Medal for his work on the James Webb Space Telescope and Chandra.

**Bruce Dean** is an optical physicist and wavefront sensing group leader at the NASA Goddard Space Flight Center. He is a member of the NASA wavefront sensing and control team for the James Webb Space Telescope and holds a patent on its primary commissioning algorithm. He was the lead optical designer for the COVIR and RIVMOS instruments and is currently vice-chair of the OSA Optical Design and Instrumentation Division, Earth, Air and Space Technical Group. He is also a recipient of the Federal Executive Bronze Award for Volunteer Service and has received the Goddard Honor Award for Engineering Achievement as well as the NASA Headquarters "Exceptional Technology Achievement Medal." He holds MS and PhD degrees in physics and mathematics from West Virginia University.

**William Hayden** is the James Webb Space Telescope lead systems engineer for the telescope element. Bill holds an MSEE from the University of Missouri-Rolla and has worked in the aerospace industry his entire career. At McDonnell-Douglas, he was on the Defense Support Program laser cross-link project where he became interested in electro-optics and electro-optical systems. This took him to NASA to work on satellite laser communications and optical science instruments, and finally on JWST, where he helped to lead development of the wavefront sensing and control subsystem and currently leads the NASA telescope systems team.

**Joseph Howard** received his PhD in optical design from The Institute of Optics, University of Rochester, and now serves as the lead optical designer for the James Webb Space Telescope. He serves on the board of directors for SPIE (2011 to 2013), as well as organizing committees for the Novel Optical Design and International Optical Design Conferences. He was recognized as an SPIE senior member in 2008.

**Ritva Keski-Kuha** is the NASA deputy optical telescope element manager for the James Webb Space Telescope at the Goddard Space Flight Center. Prior to joining JWST, she worked on numerous NASA programs developing optical coatings, mirror materials, and thin foil filters with emphasis on the extreme ultraviolet spectral region including Hubble instruments. She holds an MS and PhD in physics.